A Numerical Parametric Study on the Effectiveness of Fastener Delamination Arrest Mechanism in Composite Laminates Under Mode I Loading

Rodolfo F. V. de Melo[1,2], Maurício V. Donadon[1], Amauri Gavazzi[2]

[1]*Aeronautics and Aerospace Division, Instituto Tecnológico de Aeronáutica-ITA*
Praça Marechal Eduardo Gomes 50, 12228-900, São José dos Campos-SP, Brazil
donadon@ita.br
[2]*EMBRAER S.A.*
Av. Brigadeiro Faria Lima 2170, 12227-901, São José dos Campos-SP, Brazil
rodolfo.melo@embraer.com.br, amauri.gavazzi@embraer.com.br

Abstract. By using the Cohesive Zone Model approach and 3D solid elements to model the fastener fixation and specimen, this study aims to provide high fidelity numerical models for a double-cantilever-beam specimen configuration to investigate the effectiveness of fasteners as arrest mechanism for interface crack growth under pure mode I loading. Additionally, a parametric study was also performed to investigate the influence of joint design parameters on the specimen behavior for this loading case. Numerical results have demonstrated that a single-fastener is sufficient to completely arrest mode I delamination growth until other failure modes take place, independent of the joint design parameters. Despite this, fastener diameter, preload and type of fit have shown some influence in arrest efficiency, while adding friction penalty to the model appears to have had no significant effect under mode I loading. As a part of a more complete study for different loading cases, these results represent an incremental contribution focused on the development of design methods and tools for damage tolerant composite aerostructures.

Keywords: Bolted joints, Delamination Arrestment, Finite Elements, Cohesive Zone Models

1 Introduction

The use of composite materials in the aeronautical industry design nowadays is far from a novelty. Since the last century, their applications has constantly increased. Alongside the increasing utilization of fiber-reinforced composites in industry, understanding and predicting their failure mechanisms has had the importance potentialized. In particular, the study of interlaminar failure has demanded a lot of effort from the scientific community, since it is usually not detectable during routine checks, inspections demand special devices as ultrasound and may have a wide variety of root causes. These are some reasons why predicting it and providing quantitative data to evaluate existent methods for the arrest of its propagation are crucial.

Widely applied in metallic joints, fasteners have also been traditionally employed by the aeronautical industry in bonded or co-cured fiber-reinforced composite structures to avoid the propagation of possible delaminations and/or disbond and, consequently, to meet Aircraft Certification and damage tolerance requirements. However, little has been invested in quantifying the effectiveness of this solution as an arrest mechanism, especially concerning the assessment of the effect of several design parameters, including fastener material and diameter, preload, the minimum amount of fasteners and spacing between them. Moreover, this application has been based mostly on empirical knowledge, relying exhaustively on building block tests of coupons and subcomponents in order to validate and certificate the design solutions.

Kuen Y. Lin published recognized papers and oriented several master's theses focused on the study of the effectiveness of fasteners as delamination/disbond arrest feature. In Cheung et al. [1] and Cheung et al. [2], the authors present analytical, using the principle of minimum potential energy, and FEA models, using VCCT, for the investigation based on the use of fastener joints as mode I and mode II delamination arrest mechanism, obtaining

promising results about its effectiveness. Moreover, the researchers also observed that the fastener may completely eliminate mode I delamination, however, a pure interlaminar sliding shear crack extension mode II may still be present in the crack front. In Liu [3] and Richard and Lin [4], the previous study is extended to multiple fasteners, whereas in Lin et al. [5] the FAA technical report shows the state of the art of Lin's studies.

The study undertaken in this paper is based on the same arrest feature of Lin's work. However, the two research fronts differ based on the use of different numerical approaches. Rather than VCCT, this study makes use of the Cohesive Zone Model approach combined with 3D elements models to develop and validate high fidelity finite element models, to assess the effect of not only the fastener but also several design parameters (fastener clamping, interference class, friction) on the delamination arrest capability for mode I loading.

2 Interlaminar fracture mechanics

Delamination or interlaminar failure in fiber-reinforced laminated composites consists of the separation of two adjacent plies. The phenomenon has a significant influence on the design of composite structures, especially in the aerospace industry, the focus of this work. The reason for this concern is based on delamination high potential of harm to the structure integrity, since this failure mode may affect the stiffness and strength of the material, leading to a significant reduction in the performance of the whole composite structure.

Whitcomb [6] and Whitcomb [7] performed studies with composite laminates submitted to compressive loads analytically, experimentally and through finite element analysis to observe the influence of delamination growth in the material properties in this scenario. John Whitcomb's results shown an unstable delamination growth, which takes place when the separation of adjacent laminae in presence of compressive loads causes localized buckling. Consequently, the high interlaminar normal and shear stresses observed at the edges of the buckled region, may lead to a delamination growth. Therefore, the critical load needed to propagate the crack decreases substantially, which can easily drive the whole structure to critical fail. Then P_c decreases with the increase of delamination length and the decrease of interlaminar fracture toughness.

The other remarkable point about delamination is its wide variety of possible causes. The phenomenon may be triggered by high interlaminar stresses; however, the root cause for these stresses can be many and take place in different stages of the fiber-reinforced composite life cycle, such as during the manufacturing process, transportation, assembly, service and maintenance. Garg [8] presents a study of the delamination and the most common causes of the interlaminar stresses. In resume, it may come from: design details, like free edges, bolted joints, ply terminations and bonded/co-cured joints; impact of objects in general, from working tools and runways' debris to projectiles; matrix cracks, like off-axis ply cracks and flaws originated during the laminate's manufacturing process.

The characterization of the delamination propagation relies on general fracture mechanics theory. The total energy release rate (G) of the laminate can be decomposed into three components (G_I, G_{II} and G_{III}), which refer to the three admissible crack-extension modes of the material. Mode I is the opening mode, which represents the interlaminar tension; mode II is the forward-shear mode, which represents the interlaminar sliding shear; mode III is the parallel-shear mode, which represents the interlaminar scissoring shear.

Methods to measure the interlaminar fracture toughness (IFT), which can be defined in this case as the composite material resistance to delamination propagation, include a critical energy release rate (G_c), that when exceeded by the calculated total release rate (G), failure, i.e., delamination growth is expected. This critical energy release rate is given by the sum of its components G_{Ic}, G_{IIc} and G_{IIIc}, similar to G. Therefore, was made an effort to standardize test procedures to characterize the materials in terms of these three parameters.

2.1 DCB standard test

For the characterization of mode I interlaminar fracture toughness component, topic of this paper, the current standard for composite materials is defined in ASTMD5528–01 [9] and briefly described in this section.

The test utilizes a double cantilever beam specimen, a rectangular unidirectional composite laminate containing a thin layer of a non-stick material (usually Teflon) on its midplane. The coating forms a non-cohesive region in the interface of two plies, representing a pre-existing crack at the interface, as illustrated in figure 1.

The testing method consists of applying a vertical displacement to the end of the DCB, which has the "pre-existing crack", by means of piano hinges (as illustrated) or loading blocks bonded to the surface of each beam. The controlled displacement activates the opening mode of crack extension. From the recorded data, applied load and the crack length, the mode I critical energy release rate shall be calculated using one of three methods, however, the standard recommends the use of the modified beam theory (MBT), since is the most conservative of them.
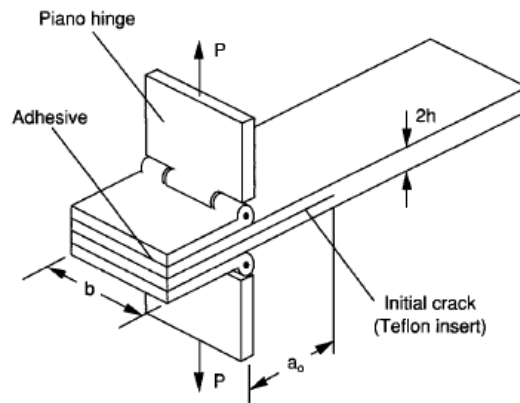
Figure 1. ASTM D5528 test configuration. Daniel and Ishai [10].

3 Cohesive zone model

Along with the evolution of Finite Element Analysis Tools, numerical methods based on interlaminar fracture mechanics were developed to study the delamination propagation through virtual testing. From the existent approaches, the Virtual Crack Closure Technique ($VCCT$) and the Cohesive Zone Model (CZM) stand out from others.

Although VCCT, recently resumed in Tabiei and Zhang [11], is the most extensively applied and validated technique in the aeronautical industry, CZM has gained space in recent years since it does not have any fracture process zone restriction, whereas VCCT requires a pre-existing crack to calculate G and the fracture process zone must be minimal in comparison to the virtual specimen dimensions.

Firstly proposed in Dugdale [12] and Barenblatt [13], the CZM, technique applied in this paper's numerical analyses, draws on a cohesive law, also known as traction-separation law, describes the mechanical behavior of the cohesive zone in face of the loading, adopting stress-based and energy-based criteria for damage initiation and propagation, respectively. The law's degradation curve is usually modeled as linear due to its good balance between computational efficiency and results accuracy. Figure 2 illustrates a scheme of the law, where S_0 is the interface strength, δ_0 and δ_F correspond to the displacement jump for the degradation initiation and the total degradation (crack opening) and K_n is the interface elastic modulus, respectively.

Note that the area below the curve in the illustration above is equal to the critical energy release rate which is mode dependent, likewise the other parameters. Therefore, distinct curves are expected for modes I, II and III. Additionally, it can be anticipated that the mixed-mode traction-separation law shall be a combination of them. In that case, a stress-based criterion is necessary to obtain the interface strength. The quadratic nominal stress criterion, or Ye's criterion, was proposed in Ye [14] and is an extensively utilized option. For the damage propagation, an energy-based criterion as Power Law (Whitcomb [15]) or B-K criterion (Benzeggagh and Kenane [16]) shall be applied.
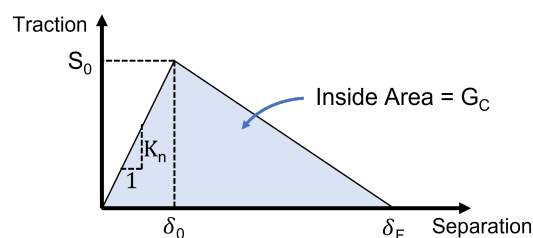
Figure 2. Linear cohesive law.

The numerical implementation of the cohesive zone model leads to the use of one of two distinct modeling techniques: cohesive interactions or cohesive elements. In the first one, the cohesive zone is given by an interaction between the upper and lower surfaces of the laminate interface, while the second method uses low- or zero-thickness elements with the cohesive zone properties,i.e., which follows the traction-separation law.

4 Numerical model

All numerical analyses presented in this paper were performed using the commercial software ABAQUS[(R)], using the dynamic explicit solver to evaluate the problem through a quasi-static approach. Since the study is focused on interlaminar failure under Mode I loading, other failure mechanisms, such as intralaminar failure, fastener failure and bearing, were not considered in the analyses. The models virtually reproduce the DCB test, described in section 3, with a specimen consisting of a rectangular unidirectional layup $[0]_{26}$ made of T800-3900 2B graphite/epoxy prepreg tapes of 0.188mm thickness (t_{lamina}), which mechanical properties are presented in Rosseau and Grant [17] and listed in Table 1. The calibrated resin properties for the co-cured interface were taken from Donadon and Arbelo [18] and Donadon and Lauda [19] and have the following values: E = 2.97GPa; G_{13} = 1.08GPa; G_{23} = 1.08GPa; σ_I = 50MPa; $\sigma_{II} = \sigma_{III}$ = 180MPa; G_{Ic} = 0.1825kJ/m^2 and $G_{IIc} = G_{IIIc}$ = 1.16kJ/m^2.

Table 1. Mechanical properties of T800-3900 2B prepreg tape.

E_{11}[GPa]	E_{22}[GPa]	G_{12}[GPa]	ν	S_{11}[MPa]	S_{22}[MPa]	S_{12}[MPa]	S_{13}[MPa]
142	7.8	3.5	0.349	2793	36	63.8	88.1

For the Mode I study, the cohesive element approach is used to implement the CZM. The elements generated have a finite thickness (t_{coh}) of 0.02mm, 10% of ply thickness, and form the cohesive zone modeled on the specimen's midplane. Other specimen relevant dimensions are: width (b) = 20mm, length (L) = 168mm and initial crack length (a_0) = 52.5mm.

The elements representing the top and lower beams of the specimen were modeled as C3D8R, while the resin layer on the midplane, as COH3D8. Despite the DCB test is pure mode I, the software requires the use of mixed-mode criteria for damage initiation and evolution. The previously mentioned Quadratic Nominal Stress Criterion and B-K Law (B-K interaction parameter = 1.75) were selected.

The whole specimen was modeled as a single part with node sharing between the inner surfaces of the arms and the cohesive layer surfaces. Nodes of top and lower edges of the beam's end (marked in red in figure 3), in which the opening displacement is applied, are restrained for translation in all directions, except z-direction (opening), and for rotation, except in y-axis. Mesh size was controlled in such a way as to obtain a balanced accuracy-processing cost ratio. Therefore, element dimension is smaller in the longitudinal direction of the double cantilever beam, while greater along transverse, i.e., y-direction.
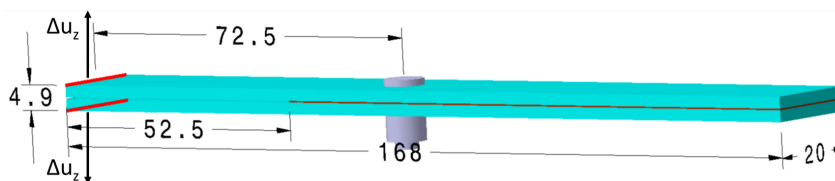
Figure 3. Specimen model schematic.

4.1 Model validation

Since the lack of experimental data for DCB tests with fasteners, the validation of the finite element model was accomplished by comparing the results of the model without fastener with a previous continuum shell-based numerical analysis performed in Donadon and Arbelo [18] and the theoretical solution based on the principle of minimum potential energy described in Donadon [20].

For that validation model, mesh size was maintained the same for the area of cohesive zone where element degradation is observed during the simulation. After a convergence analysis, it was defined for the cohesive layer a number of 2028 elements with 0.2mm x 3.33mm size and 132 elements with 2mm x 3.33mm size. The whole model consists of 22848 elements.

Figure 4 shows no alarming divergence between the curves, validating the model concerned. However, some differences may be pointed out. The different ratio for elastic response in the theoretical solution compared to the finite element analyses may be explained by the effects of geometrical non-linearities observed in the three-dimensional FE model and missing in the analytical formulation, which is based on the beam theory.
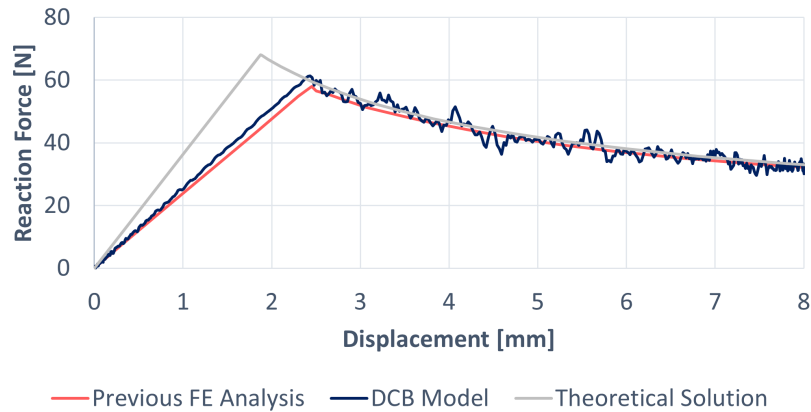
Figure 4. Numerical model validation.

4.2 Fastener modeling

The study selected H-LITE HST10 pins in Ti 6AL-4V (E = 114GPa; ν = 0.33) combined with HST1094 collars in 302 Stainless Steel (E = 193GPa; ν = 0.25). Dimensions were taken from the catalogues Lisi [21] and Lisi [22] respectively. To achieve more accuracy in the output results, solid elements were used to represent the fastener. Its model consists on pin and collar fixed together by means of a tie constraint. Both components were modeled as C3D8R, 8-node linear brick with reduced integration elemnts. The pin part is composed of 4764 elements, while the collar part contains 1404. The mesh control set a maximal element size of 0.5mm for both components. Contact interactions were defined for specimen-fastener interfaces with "hard" contact for normal behavior and frictionless, except where specified, for tangential behavior.

Fastener preload and interference fit were two conditions that could not be entirely simulated in the Explicit solver. Since the features are only available in ABAQUS$^{(R)}$ Standard, for the models with one of the two conditions, the analyses were run first using the Implicit solver to apply the condition. Then the model and its final state were imported to Abaqus Explicit, where the DCB test where simulated. Table 2 summarises the conditions modeled in this study.

Table 2. Models summary.

Run	Fastener diameter [mm]	Number of fasteners	Friction coef.	Preload [N]	Interference
S1	-	0	0	0	-
S2	4.7625	1	0	0	-
S3	4.7625	1	0.3	0	-
S4	4.7625	2 (20mm spacing)	0	0	-
S5	4.7625	1	0	0	+6.3% (clearance)
S6	4.7625	1	0	1320	-
S7	4.7625	1	0	0	-5% (interference)
S8	4.7625	1	0.3	0	+5% (clearance)
S9	4.7625	1	0.3	1320	+5% (clearance)

5 Results

A general assessment of the simulations results presented in figure 5 confirms that fasteners are effective in containing delamination growth regardless of the design variables applied. However, the study has shown some efficiency differences, when varying some parameters.
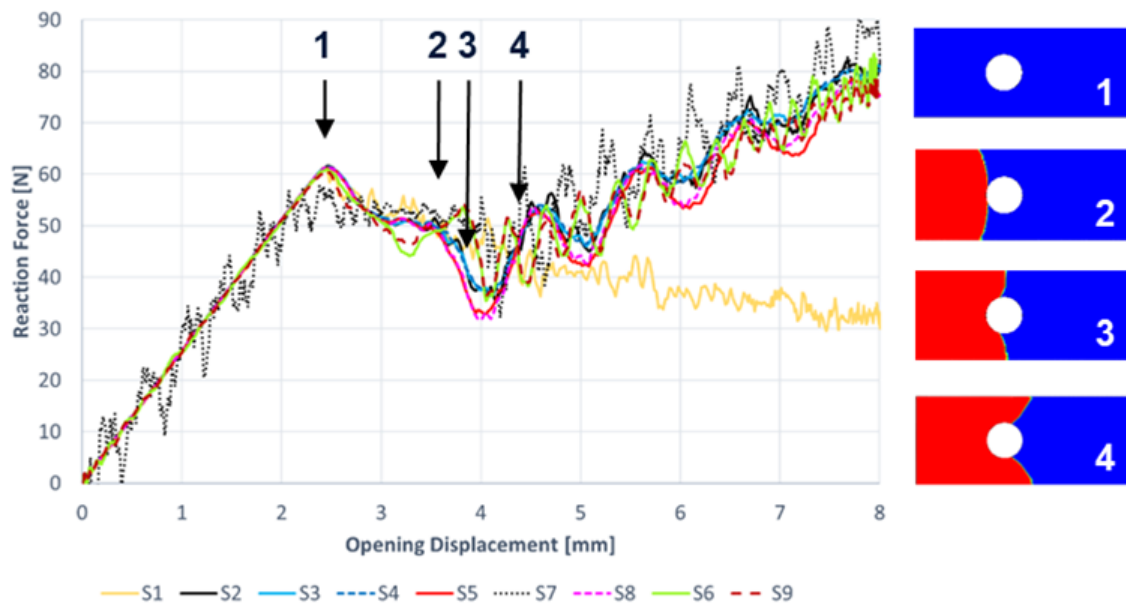
Figure 5. Simulations results: Reaction Force x Opening Displacement.

Curve S2 (fastener base model) indicates that delamination propagates until reaches the fastener, then the reduction in the specimen effective width leads induces the reaction force to sink until the fastener arrest effect takes place and a continuum increase in force magnitude is observed. This behavior is seen in all other simulations with fastener, but it is noticeable in rounds S6 and S7 that preload and interference fit may minimize this reduction in reaction force leading to more efficient joints. Preload even maximizes the fastener efficiency by starting crack arrestment before the delamination front reaches the joint.

From curve S3, it can be inferred that, despite relevant for shear modes, friction appears to not influence delamination arrestment. The same behavior is observed for the round S4, in which a second fastener is placed 20mm from the first in series. Data confirms the expectation, since the first fastener completely contains the crack propagation and the second one would only actuate, if the crack front reached the fastened joint.

The offset between curves S2 and S5 indicates a greater sink in reaction force and consequently, a delay in crack arrestment for the model with a clearance fit in the mechanical joint. Since the hole diameter is greater than the pin nominal diameter, the effective width reduction effect already mentioned in this paper increases. On the other hand, the interference fit delivers a more efficient joint, since the reduction in the reaction force magnitude is not observed in curve S7. Another interesting observation is that curves S5 and S8 have the exact behavior, confirming that friction has no relevant influence on the delamination arrestment for mode I loading.

Finally, the study simulated the most typical set in real fastened joints for fiber-reinforced composites. Curve S9 shows that preload may hinder the negative effect of the clearance fit, representing a joint almost so efficient as in curve S6.

6 Conclusions

The analyses results assessment above led to the understanding that only one fastener, independently of the design variables, is sufficient to contain delamination growth, since the propagation is completely arrested until another failure mode takes place. The design parameters slightly affect the joint efficiency. In this sense, friction penalty appears to have no significant effect on delamination propagation, while clearance leads to a delay in the crack arrestment. Preload, especially, and interference fit arise as parameters with a positive impact on the fastener efficiency.

Finally, the study confirms the effectiveness of fasteners as a delamination arrest mechanism for mode I loading, being in accordance with previous researches in the literature. As an incremental contribution to this field of study, the paper also shows how the design parameters may affect the efficiency of the joint in containing the interlaminar failure.

Authorship statement. The authors hereby confirm that they are the sole liable persons responsible for the authorship of this work, and that all material that has been herein included as part of the present paper is either the property (and authorship) of the authors, or has the permission of the owners to be included here.

References

[1] C. Cheung, P. Gray, K. Li, and G. Mabson. Analysis of fasteners as disbond arrest mechanism for laminated composite structures. In *51st AIAA/ASME/ASCE/AHS/ASC Structures, Structural Dynamics, and Materials Conference 18th AIAA/ASME/AHS Adaptive Structures Conference 12th*, pp. 3024, 2010.

[2] C. Cheung, P. Gray, and K. Lin. Fastener as fail-safe disbond/delamination arrest for laminated composite structures. In *Proceedings of the 18th International Conference on Composite Materials (ICCM18), Jeju Island, Korea*, 2011.

[3] W. Liu. Analysis of delamination arrest fasteners in bolted-bonded composite structures. Master of science in aeronautics and astronautics, University of Washington, 2014.

[4] L. Richard and K. Lin. Delamination/disbond arrest features in aircraft composite structures. *Ed. William E. Boeing, Department of Aeronautics and Astronautics, Seattle, WA*, vol. 98195, 2014.

[5] K. Lin, L. Richard, and C. Cheung. Delamination/disbond arrest features in aircraft composite structures. Technical Report DOT/FAA/TC-18/5, Federal Aviation Administration, 2018.

[6] J. Whitcomb. Finite element analysis of instability related delamination growth. *Journal of Composite Materials*, vol. 15, n. 5, pp. 403–426, 1981.

[7] J. Whitcomb. Parametric analytical study of instability-related delamination growth. *Composites Science and Technology*, vol. 25, n. 1, pp. 19–48, 1986.

[8] A. Garg. Delamination - a damage mode in composite structures. *Engineering Fracture Mechanics*, vol. 29, n. 5, pp. 557–584, 1988.

[9] ASTMD5528–01. Standard test method for mode i interlaminar fracture toughness of unidirectional fiber-reinforced polymer matrix composites. ASTM International, 2007.

[10] I. Daniel and O. Ishai. *Engineering Mechanics of Composite Materials: Second Edition*. Oxford University Press, 2006.

[11] A. Tabiei and W. Zhang. Composite laminate delamination simulation and experiment: A review of recent development. *ASME Applied Mechanics Reviews*, vol. 70, n. 3, 2018.

[12] D. Dugdale. Yielding of steel sheets containing slits. *Journal of the Mechanics and Physics of Solids*, vol. 8, pp. 100–104, 1960.

[13] G. Barenblatt. The mathematical theory of equilibrium cracks in brittle fracture. *Advances in Applied Mechanics*, vol. 7, pp. 55–129, 1962.

[14] L. Ye. Role of matrix resin in delamination onset and growth in composite laminates. *Composites Science and Technology*, vol. 33, n. 4, pp. 257–277, 1988.

[15] J. Whitcomb. Analysis of instability-related growth of a through-width delamination. Technical report, NASA Langley Research Center, 1984.

[16] M. Benzeggagh and M. Kenane. Measurement of mixed-mode delamination fracture toughness of unidirectional glass/epoxy composites with mixed-mode bending apparatus. *Composites Science and Technology*, vol. 56, n. 4, pp. 439–449, 1996.

[17] C. Rosseau and P. Grant. *Composite structures: theory and practice - STP 1383*. ASTM International, 2000.

[18] M. Donadon and M. Arbelo. Relatório cienfífico parcial período novembro/2015 a julho/17 - projeto fapesp 2015/16733-2. Technical report, Instituto Tecnológico de Aeronáutica, 2015.

[19] M. Donadon and D. Lauda. A damage model for the prediction of static and fatigue-driven delamination in composite laminates. *Journal of Composite Materials*, vol. 49, n. 16, pp. 1995–2007, 2014.

[20] M. V. Donadon. Lecture notes ae-727: Analysis and design of composite structures, 2019.

[21] Lisi. Hi-lite pin protruding shear head titanium 1/16 grip variation. Torrance, California, U.S., 2017.

[22] Lisi. Hi-lite collar stainless steel 1/16 grip variation, shear application for use on standard and 1/64 oversize hi-lite pins. Torrance, California, U.S., 2019.